J Mater Sci (2007) 42:4521–4529
DOI 10.1007/s10853-006-0471-3

Crystal morphologies in thin films of PEO/PMMA blends

B. C. Okerberg · H. Marand

Received: 24 March 2006 / Accepted: 25 May 2006 / Published online: 15 February 2007

Abstract Crystallization in thin films of poly(ethylene oxide) in blends with poly(methyl methacrylate) has been studied. The film thickness is fixed at 120 nm, while the blend composition, PMMA molar mass, and crystallization temperature are varied. Blends with a composition of 50/50 (wt% PEO/wt% PMMA) exhibit a variety of morphologies that are highly dependent on PMMA molar mass and crystallization temperature. A needle morphology not previously reported in this system is also observed. For 40/60 blends, dendrites and DBM are observed at high PMMA molar mass. At low PMMA molar mass, a number of morphologies are observed over small changes in the experimental controls. In 35/65 blends, dendritic growth is observed with sidebranches at 45° and 90° to the dendrite trunk at low undercooling and only at 90° for larger undercooling. For 30/70 blends, dendritic growth is observed over a large range of PMMA molar mass and crystallization temperature. Maps demonstrating the role of the control parameters on morphological development are reported. The observed morphologies are believed to result from the combined effects of the lack of crystallizable chains at the growth front, low dimensionality, rejection of non-crystallizable chains, and variation of the effective levels of noise and/or anisotropy.

B. C. Okerberg
Department of Materials Science and Engineering, Virginia Tech, Holden Hall, Blacksburg, VA 24061, USA
e-mail: bokerber@vt.edu

H. Marand (✉)
Department of Chemistry, Virginia Tech, Davidson Hall, Blacksburg, VA 24061, USA
e-mail: hmarand@vt.edu

Introduction

Pattern formation during crystallization has been studied for a number of years. Many studies have focused on dendritic crystallization of metals and small molecules because these dendritic microstructures are known to play a large role in the resulting mechanical properties [1]. Pattern formation in facet-forming materials, such as polymers, has been studied in less detail, although early studies have shown that the presence of facets does not necessarily preclude pattern formation [2–4]. One of the outstanding problems in pattern formation is an understanding of the processes by which substances that normally crystallize in faceted manner can be driven to crystallize in non-equilibrium, diffusion-limited morphologies.

In general, faceted crystals have atomically smooth interfaces that grow through a layer-by-layer mechanism, such as secondary surface nucleation (nucleation-limited growth). On the other hand, non-faceted crystal morphologies involve rough interfaces characterized by many favorable sites for atom attachment. In the latter case, crystal growth is controlled by diffusion of heat or mass away from the melt-crystal interface (diffusion-limited growth). Jackson suggested that the nature of the interface (faceted vs. non-faceted) correlates with the magnitude of the entropy of fusion [5]. Smooth interfaces are observed in materials exhibiting large entropies of fusion (polymeric materials), while rough interfaces are typically found in metals and other materials with small entropy of fusion.

Metals typically solidify from the melt in a dendritic manner. Dendrites result from a thermal or solutal diffusion field surrounding the crystal and their sym-

metry reflects the crystallography of the unit cell (for cubic materials, sidebranches typically form at 90° to the dendrite trunk). Some small anisotropy in the surface energy is required for the formation of the dendritic pattern [6]. One of the important length scales in dendritic growth is the diffusion length, $\delta = D/V$, where D is the heat or mass diffusion coefficient and V is the crystal growth velocity. This length represents the characteristic distance over which impurities (or heat) are rejected from the growing crystal.

Metallic dendrites are often difficult to study experimentally because they are not transparent and crystal growth rates are extremely large. These experimental difficulties have been overcome in studies of substances such as succinonitrile [7, 8], pivalic acid [9], ammonium chloride [10], ice [11–13], xenon [14–16], camphene [17], and ammonium bromide [18]. These model systems have allowed for measurements of the sidebranching spacing, tip radius, and growth velocity, which have subsequently been used to test existing theories of dendritic growth [7]. For detailed discussions of the fundamental aspects of dendrite formation, the reader is referred to papers by Langer [19], Billia et al. [20], and Glicksman et al. [21].

As discussed previously, polymeric materials usually crystallize in a faceted manner. These faceted crystals take the form of lamellae, which are single crystals with ribbon or plate-like shapes, resulting from highly anisotropic attachment kinetics. Lamellae are usually organized in a spherulitic fashion when crystallization takes place from the pure melt or from a concentrated solution [22]. In contrast, crystallization from dilute solution leads to isolated single crystal lamellae at small undercooling and to dendritic patterns at larger undercooling [23–25]. Recent studies of crystallization in thin films have confirmed the ability of polymeric materials to crystallize in a variety of non-spherulitic morphologies [26–35].

In addition to faceted single crystals, spherulites, and dendrites, other morphologies, such as the dense-branched morphology (DBM) [36, 37] have been encountered in crystal growth experiments. The dense-branched morphology (DBM) is usually observed in low anisotropy conditions and is characterized by frequent splitting of the growth tip and a lack of pronounced geometrical order [38, 39]. While this morphology is rarely reported experimentally, it has generated some controversy over its classification as a true morphology [40]. Another problem with use of the term ''DBM'' is that some of the reported examples are single crystals while others are polycrystalline [30, 36]. This is an important distinction because in the former case, diffraction patterns show pronounced crystallographic order (despite the lack of geometrical order), while in the latter case, the diffraction pattern reveals polycrystalline textures. In polymeric materials, the reported dense-branched morphologies are almost exclusively single crystals [26, 30, 32].

The spherulitic growth morphology has also generated significant confusion in the literature. In some cases, such as selenium [41], lead glasses [42], sulfites in gels [43], and lamellar eutectics [44], the term spherulite is used to describe a polycrystalline pattern with a spherical envelope consisting of a lamellar microstructure. In polymeric materials, the term spherulite generally refers to an aggregate of single crystal lamellae that originates from a single primary nucleus and achieves spherical symmetry through repeated low angle branching and splaying [45, 46]. Branching at the lamellar level is usually associated with the occurrence of screw dislocations [47].

Goldenfeld proposed that spherulites are three-dimensional representations of the dense-branched morphology [39]. Although this statement may be generally true, the situation is more complicated for polymers than for small organic or inorganic molecules. In polymeric materials, two types of instabilities may occur at the growth front. In the first case, instability at the growth tip of a thin polymer lamella, often resulting from mechanical stress, leads to the generation of a screw dislocation and eventually to the formation of a lamellar stack. Following the reasoning of Keith [48], Keith and Padden [49] and Schultz [50], these single lamellae are too thin to lead to a Mullins-Sekerka growth instability. In contrast, once lamellar stacks (fibers) reach lateral dimensions commensurate with the diffusion length, a growth instability leads to non-crystallographic branching (splitting of the growth envelope into separate fibers). More recently, tip-splitting in the plane of crystal growth has been observed for a number of polymeric materials in thin film geometries [26, 27, 30, 32–34]. This type of instability has been interpreted to result from the lack of crystallizable chains at the growth front.

The addition of impurities may also result in instabilities of the growth front. In many bulk polymer systems, rejection of non-crystalline components occurs between the crystalline lamellae as evidenced by linear growth kinetics and an increased long spacing [51]. In some systems, these impurities are rejected entirely from the crystal front, resulting in a cellulation of the growth front [48]. Confinement in thin film geometries may lead to rejection of impurities in the plane of the growing crystal and instability of the growth front [49]. These instabilities may result in a

breakdown of the normally faceted growth morphology into a number of other morphologies.

A number of theoretical studies of transitions between morphologies have been reported [52–54]. These morphological transitions have been observed upon changes in some control parameter such as the effective anisotropy or the undercoooling. Experimentally, these transitions are commonly reported in Hele-Shaw experiments [36] but have been more elusive in studies of phase transitions (such as crystallization) [55–57]. Often, only a single morphology is observed, suggesting that transitions between morphologies may require large changes in a control parameter. These large changes in experimental conditions are often not possible in standard experiments due to a variety of factors such as rapid nucleation at large undercooling and large crystal growth rates. We anticipate here that polymeric materials may provide some insight into these transitions because of their relatively small rates of nucleation and crystal growth, large crystallization window, and tunable diffusion coefficients (through changes in the molar mass).

Ferreiro and coworkers have recently reported morphological transitions in thin film blends of poly(ethylene oxide) (PEO) and poly(methyl methacrylate) (PMMA) upon changes in the blend composition [34, 35]. In this system, the PEO crystallizes and the non-crystallizable PMMA chains are rejected from the growth front. It is important to note that in polymer blends such as PEO/PMMA, the two components form a single phase in the liquid state and the phase diagram consists of a single crystalline phase (not two phases as is typical of binary metallic systems) [58]. The observed crystal morphologies were found to be similar to those generated by a phase field model where the effective anisotropy was varied. Montmorillonite clay was used as a nucleating agent in these experiments and the amount of clay in the system was shown to have a dramatic effect on the observed morphology.

In the present work, we report further studies of morphological development in thin films of PEO/PMMA blends. The PEO content is varied between 50 and 30 wt% since a number of morphological transitions were reported over this composition range [34, 35]. Clay was not used in our study to minimize the number of experimental variables. The focus of this paper is twofold: first, to identify the different morphologies in PEO/PMMA blends as well as their location in parameter space (morphological maps), and second, to provide directions for further study of morphological development and pattern formation in polymeric systems. The effects of the control parameters (blend composition, PMMA molar mass, crystallization temperature) on morphological development are also discussed.

Experimental

Poly(ethylene oxide) and poly(methyl methacrylate) were obtained either from Scientific Polymer Products and Polymer Laboratories and used as received. The molar mass and polydispersities are reported in Table 1. In this study, crystallized blend samples are referred to by the PMMA molar mass (names shown in Table 1).

The PEO and PMMA were dissolved in HPLC-grade 1,2-dichloroethane overnight and then stirred for 2 h before use. The polymer concentration in solution was approximately 1.25 wt% and the composition of the blend was varied from 50 to 30 wt% PEO. Silicon wafers (100) were cleaned with a hot solution of 70 vol% sulfuric acid and 30 vol% hydrogen peroxide for 2 h to create a hydrophilic surface. After cleaning, the wafers were rinsed with deionized water and blown dry with nitrogen.

Before spin-coating, the wafers were rinsed with HPLC-grade 1,2-dichloroethane and spun dry. The polymer solutions were then spin-coated onto the silicon wafer at approximately 1,000 rpm. The resulting dry film thickness was approximately 120 nm, as determined using a JA Woollam spectroscopic ellipsometer. The film thickness is not affected dramatically by the PMMA molar mass, but is highly sensitive to the concentration of polymer in solution. Blend composition was also shown to have a moderate influence on film thickness (110 nm for (30/70) and 130 nm for (50/50) PEO/PMMA blends). Studies carried out with blend films of a specific composition but slightly

Table 1 Weight-average molar mass and polydispersities of polymers used in this study

Material	M_w (g/mol)	M_w/M_n
PEO	101,200	1.04
PMMA5	4,900	1.10
PMMA7	6,880	1.07
PMMA12	12,000	1.08
PMMA13	12,500	1.03
PMMA17	16,700	1.06
PMMA18	17,900	1.10
PMMA30	30,490	1.02
PMMA53	52,700	1.08
PMMA68	68,200	1.13
PMMA101	101,000	1.09

different thickness (±30 nm) showed no significant change in morphology. Spin-coated samples were then dried under vacuum at 60 °C for 2 h and then transferred to a Linkam heating stage. The samples were heated to 80 °C for 1 min (to melt any crystals formed during drying) and crystallized under nitrogen. In this study, we report the crystallization temperature rather than undercooling because the actual undercooling is not precisely known due to difficulties associated with determination of the equilibrium melting temperature in polymeric crystals [59]. The approximate range of undercooling, $\Delta = T_m - T_c$, used is this study is 6–56 °C, assuming a constant equilibrium melting temperature of 76 °C since the Flory–Huggins interaction parameter is approximately zero [60]. An Olympus BH-2 reflected light microscope equipped with a Cohu CCD camera was used to observe the crystal growth morphology. The image contrast was digitally enhanced to show the morphologies more clearly.

Results

(50/50) PEO-PMMA blends

A wide range of morphologies were observed in studies of the 50/50 blends. These morphologies are highly dependent on the PMMA molar mass and crystallization temperature. Only the effect of the crystallization temperature is discussed here (varying the PMMA molar mass results in similar changes, especially for low PMMA molar mass). At small undercooling and low PMMA molar mass (near PMMA12), dendritic (D90) morphologies are observed, as shown in Fig. 1a. These dendrites have sidebranches at 90° to the dendrite trunk. Increasing the undercooling results in the formation of the dense-branched morphology (DBM), as shown in Fig. 1b. The dendrite arms and the DBM branches continuously decrease in width with increasing undercooling. Increasing the undercooling beyond the DBM regime results in the formation of a stacked-needle (SN) morphology. The stacked-needle morphology is shown in Fig. 1c. Further increases in the undercooling results in a needle (N) morphology, as shown in Fig. 1d. The needle morphology exhibits a relatively low frequency 90° sidebranching. Increased branching and bending of these needles is observed at larger undercooling. Eventually, the needles become very dense with a circular envelope. At very low molar mass and large undercooling, these dense-needled morphologies appear very similar to spherulites commonly observed in polymeric systems. Preliminary in-situ observations of morphological transitions also indicate that many of the observed transitions (excluding transitions involving stacked-needles) are of the second-order variety (continuous velocity at the transition point).

(40/60) PEO-PMMA blends

A number of morphologies are also observed in 40/60 blends. Crystallization at large undercooling and high PMMA molar mass produces dendrites with 90° sidebranching (D90). At smaller undercooling, a dense-branched morphology is observed.

Morphologies observed at high undercooling for blends containing low molar mass PMMA appear to be intermediates between dendrites, needles, and DBM and are difficult to categorize. Each of these morphologies exists over a limited range of conditions.

(35/65) PEO-PMMA blends

For 35/65 blends, the morphologies are deeply in the dendritic regime. At large undercooling, the D90 morphology is observed across the range of PMMA molar mass studied. An example of the D90 morphology for this blend composition is shown in Fig. 2a. The lower undercooling region is dominated by dendrites with a large number of 45° sidebranches, especially for larger PMMA molar mass. Some of the sidebranches also grow at 90° near the transition temperature. An example of this morphology (D45) is shown in Fig. 2b. The DBM morphology is still occasionally observed at low PMMA molar mass.

The density of well-developed (independent) sidebranches decreases with increasing PMMA molar mass but appears to be relatively independent of the crystallization temperature over the relatively narrow temperature window used in this study.

(30/70) PEO-PMMA blends

The observed morphologies in 30/70 blends are entirely dendritic. However, because of the relatively slow crystal growth rates (less than 10^{-4} μm/s) at small undercooling, the region above the observed dendritic region has not been extensively studied. The D45 morphology is observed at low undercooling in low PMMA molar mass samples. As in 35/65 blends, the density of developed sidebranches decreases significantly with increasing PMMA molar mass.

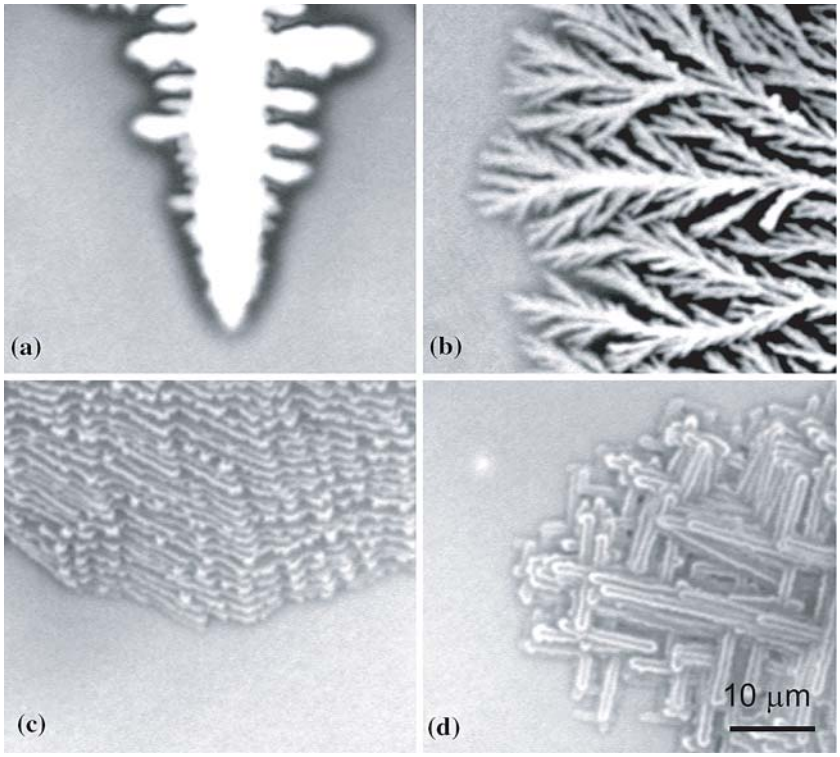

Fig. 1 Optical micrograph of morphologies observed in a 50/50 samples: (**a**) Dendrite (D90)—PMMA16, T_x = 58 °C, (**b**) Dense-Branched Morphology (DBM)—PMMA101, T_x = 50 °C, (**c**) Stacked Needles (SN)—PMMA101, T_x = 42 °C, (**d**) Needles (N)—PMM101, T_x = 40 °C

Morphological maps

Morphological maps for 50/50, 40/60, 35/65, and 30/70 blend compositions are reported as a function of crystallization temperature and PMMA molar mass in Fig. 3–6, respectively. Morphologies are not reported for cases where the growth rate was prohibitively slow. It is interesting to note that the morphology boundaries mirror the expected evolution of the PMMA and PEO/PMMA glass transition temperature as a function of increasing PMMA molar mass.

Fluctuations in film thickness within and among samples, as well as variations in blend composition and polymer concentration result in slightly different transition temperatures for different samples. This is particularly true for blends containing low PMMA molar mass. Despite the difficulty in determining exact transition temperatures, the same trend in morphologies is always observed in different samples, and the reported maps can be used as a general guide for determining where the different morphologies are observed.

Discussion

Morphological development in polymers

Several important issues about pattern formation in polymeric systems versus small molecules or metals must be addressed before any detailed discussion of the

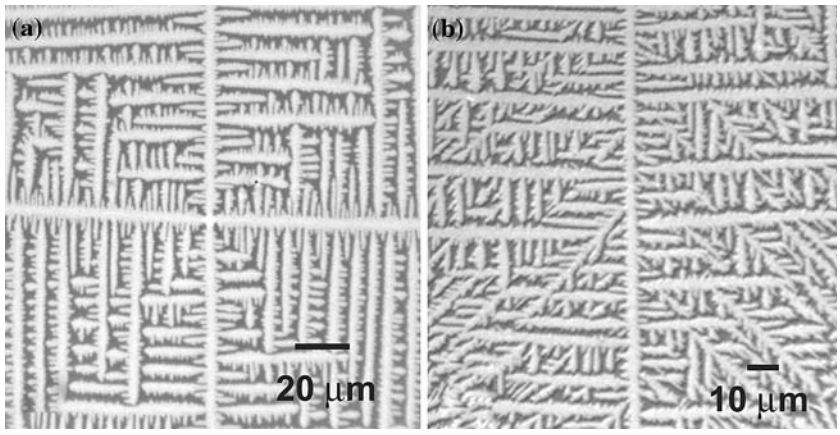

Fig. 2 (**a**) Optical micrograph of the D90 morphology observed in a 35/65 PMMA101 sample crystallized at 37 °C, (**b**) Optical micrograph of the D45 morphology observed in a 35/65 PMMA68 sample crystallized at 41 °C

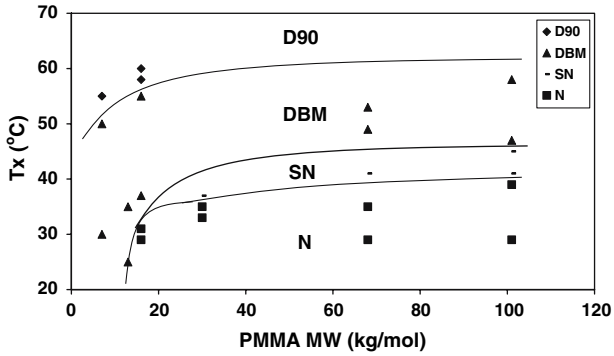

Fig. 3 Morphological map for 50/50 blends as a function of PMMA molar mass and crystallization temperature

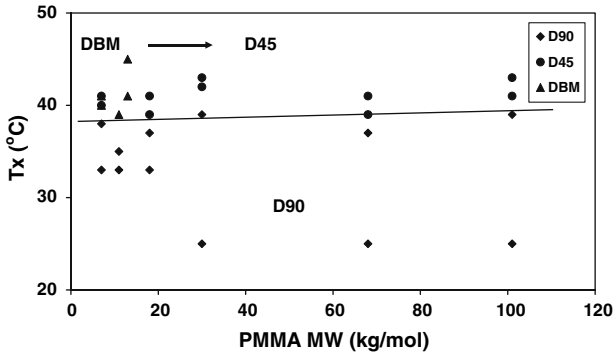

Fig. 5 Morphological map for 35/65 blends as a function of PMMA molar mass and crystallization temperature

observed morphologies can be given. Polymer crystals form by a chain folding mechanism and their thickness decreases with increasing undercooling [61]. At low undercooling, crystallization is very slow but requires a large amount of material to form thick crystals. In addition, the crystalline phase is typically denser than the amorphous phase, resulting in a depletion zone ahead of the growth front [30]. The combined effects of crystal thickness requirements and density change during crystallization may play an important role in pattern formation in these systems. Convection effects in polymer melts are negligible because of their large viscosity. Another interesting feature of polymeric dendrites is that isothermal coarsening does not occur to any significant degree due to limited surface diffusion and the inability of new crystallizable material to reach the crystal (diffusion is slow and the PEO crystal is essentially enclosed in a glassy PMMA-rich phase). These features will be discussed further in a subsequent publication [62].

In the PEO/PMMA system, attractive interactions with the substrate may result in a relatively high glass transition temperature near the substrate. In this case, crystals grow preferentially near the air/film interface due to enhanced mobility [63]. As a result of this gradient in glass transition temperature [64], the effective film thickness for crystallization may be much less than the actual film thickness. Hence, the non-crystalline PMMA component is likely rejected in the plane of crystal growth [65]. The result of these constraints (low dimensionality, rejection of PMMA, and depletion in PEO) is that the growth front of a faceted crystal becomes unstable and new morphologies develop. The selection of the new growth morphology depends on the interplay of these constraints as well as the effective levels of noise and anisotropy [38].

It is also important to point out that the length scales related to sidebranching in the dendritic morphologies are very small compared to the crystal width observed optically in Figs. 1 and 2. Using approximate values of the diffusion coefficient (10^{-12} cm^2/s) and growth rate (10^{-8} cm/s), the diffusion length is on the order of 10^{-4} cm and the corresponding Mullins-Sekerka instability length is on the order of 10^{-6} cm (~10 nm). These values are supported by AFM observations of the growth tip and will be discussed in more detail in a subsequent publication [62]. These length scales are beyond the resolution of the images presented in

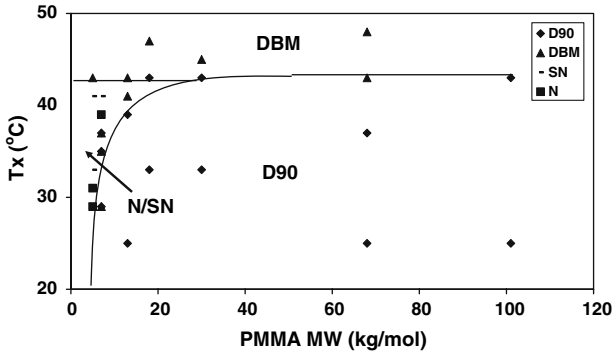

Fig. 4 Morphological map for 40/60 blends as a function of PMMA molar mass and crystallization temperature

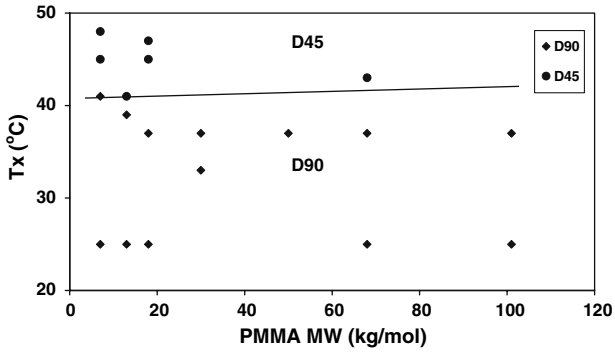

Fig. 6 Morphological map for 30/70 blends as a function of PMMA molar mass and crystallization temperature

Figs. 1 and 2, meaning that the observed crystal width actually consists of a collection of many generations of sidebranch growth.

Needles (N)

The term ''needle'' is often used to describe a dendritic crystal with no sidebranching. The use of the term ''needle'' in this study refers to morphologies that resemble dendrites because of the 90° sidebranching but have a relatively small number of branches. The 90° sidebranches, observed in needles and dendrites (see Section on dendrites), indicate a crystallographic relationship [66] between the needle/trunk and sidebranch. This relationship also indicates that the needles (and dendrites) are flat-on with the fold surface parallel to the substrate (i.e. vertical chain axis with respect to the substrate). However, the reason that sidebranching is suppressed at high mobility (50/50 blends) is not clear, but may be related to the crystal's relatively large growth rate. Detailed studies of the growth tip are not currently possible due to the small size and rapid growth rates of these needles.

Needle crystals morphologies have scarcely been reported in morphological studies. In polymers, needle-like morphologies have been observed in polypropylene but these are a result of specific epitaxial growth conditions [67, 68], which are not relevant to the current study. Shibkov and coworkers have reported similar morphologies in studies of ice crystals growing from supercooled water [57]. Ice is similar to polymer lamellae in that the crystals often grow in two-dimensions (in the basal plane) with a large anisotropy in the molecular attachment kinetics. In our studies, the needles' sidebranching and spatial density increases with increasing undercooling, as also reported by Shibkov et al. [57]. The flipping of the D90/DBM boundary between Figs. 3 and 4 may indicate that the needles are kinetic dendrites while the D90 morphology is governed by the surface tension. A similar explanation was proposed by Shibkov for supercooled water [11, 57]. More studies of similar materials would be useful to determine if the needle morphology is common in materials with large anisotropies of attachment kinetics or if the two-dimensionality of the crystal is critical for the observation of the needle morphology.

Stacked-needles (SN)

The stacked-needle morphology is observed at slightly higher temperatures than the needle morphology. This morphology is rarely discussed in crystallization experiments. Keith reported crystal aggregates in thin films of isotactic polystyrene that appear somewhat similar to the SN morphology but no mechanism for their formation was described [see Fig. 4 in ref. 48]. We speculate that this morphology is comprised of needles tilted toward the film surface and hope to conduct detailed X-ray diffraction experiments in the future to resolve this issue.

Dense-branched morphology (DBM)

In theoretical studies of crystal morphologies, DBM is normally observed at large undercooling and/or small anisotropy of the surface energy [69]. Xu and coworkers have suggested that the observation of DBM in isotactic polystyrene is a result of the decrease in the anisotropy associated with the large undercooling [70]. Ben-Jacob and coworkers have also indicated that the anisotropy of the surface energy in polymeric materials is very small, resulting in DBM rather than dendrites [36]. Since DBM is frequently observed during crystallization of thin polymer films, such a mechanism for DBM formation is indeed plausible. However, such a suggestion relies on the existence of a mechanism that reduces the anisotropy of molecular attachment. This anisotropy is required to stabilize faceted interfaces normally associated with polymer crystallization. In the present case, this mechanism may be related to the rejection of PMMA from the interface [24, 62].

In addition, noise may play an important role for the development of DBM and destabilization of dendritic morphologies, given that we observe DBM in situations where the noise level is expected to be large (high PEO content blend with low Tg). This suggestion has been frequently proposed in theoretical treatments and can not be ruled out [69, 71].

Dendrites (D)

Dendritic growth in polymers has also been reported in highly constrained environments [30, 31, 34, 35]; however, these dendritic morphologies are reported much less frequently than DBM. This observation is initially surprising given that dendrites are considered to be the normal mode of pattern formation in metallic and small molecule systems. For reasons already discussed, DBM is expected to be the general mode of crystallization in thin polymer films, with dendrites occurring only under the proper growth environments (low noise levels and slow crystal growth).

The transition from 45 to 90° sidebranching with increasing undercooling is not well understood in this

system, but may be related to the (010)/(120) growth front transition noted by Marentette et al. [72]. Another possibility is the competition between surface tension anisotropy and anisotropy in molecular attachment kinetics as discussed by Liu and Goldenfeld [73]. This competition will be described in more detail in a subsequent publication [74].

Conclusions

The effects of blend composition, PMMA molar mass, and crystallization temperature on the observed crystal morphology have been studied in thin film blends of PEO/PMMA. A number of morphologies have been reported, including dendrites (D), dense-branched morphology (DBM), needles (N), and stacked-needles (SN). Morphological maps demonstrating the roles of the various control parameters (blend composition, PMMA molar mass, and crystallization temperature) on the observed morphology are reported. The blend composition, undercooling, and to a minor extent the PMMA molar mass play important roles in morphological selection. The needle and stacked-needle morphologies are reported for the first time in this system. In addition, a change in the direction of sidebranching for dendritic crystals has been observed. These results provide a number of immediate directions for detailed studies of dendritic growth and morphological transitions in polymeric systems.

Acknowledgements The authors thank the donors of the Petroleum Research Fund, administered by the American Chemical Society (Grant ACS PRF #34069-AC7), for partial support of this work. The authors would also like to thank Jack Douglas and Vincent Ferreiro for helpful discussions.

References

1. Kurz W, Fisher DJ (1998) Fundamentals of solidification. Trans Tech Publications, Switzerland
2. Ben Amar M, Pomeau Y (1988) Europhys Lett 6(7):609
3. Maurer J, Bouissou P, Perrin B, Tabeling P (1989) Europhys Lett 8(1):67
4. Adda Bedia M, Ben Amar M (1991) In growth and form. Plenum Press, New York, pp 187–199
5. Jackson KA (1958) Liquid metals and solidification ASM. Cleveland, p 174
6. Kessler DA, Koplik J, Levine H (1984) Phys Rev A 30:2820
7. Glicksman ME, Schaefer RJ, Ayers JD (1976) Metall Trans A 7:1747
8. Huang SC, Glicksman ME (1981) Acta Metall 29:701
9. Dougherty A, Gunawardana A (1994) Phys Rev E 50(2):1349
10. Honjo H, Otha S, Sawada Y (1985) Phys Rev Lett 55(8):841
11. Shibkov AA, Zheltov MA, Korolev AA, Kazakov AA, Leonov AA (2005) J Cryst Growth 285:215
12. Koo K, Ananth R, Gill WN (1991) Phys Rev A 44(6):3782
13. Tirmizi SH, Gill WN (1989) J Cryst Growth 96:277
14. Bisang U, Bilgram JH (1996) Phys Rev E 54(5):5309
15. Singer HM, Bilgram JH (2004) Phys Rev E 70:031601
16. Singer HM, Bilgram JH (2005) J Cryst Growth 275:e243
17. Rubinstein ER, Glicksman ME (1991) J Cryst Growth 112:97
18. Honjo H, Sawada Y (1982) J Cryst Growth 58:297
19. Langer JS (1980) Rev Mod Phys 52(1):1
20. B Billia, R Trivedi (1993) Handbook of Crystal Growth, Fundamentals: transport and stability, vol. 1B. Elsevier Science Publishers B.V., New York, pp 899–1073
21. Glicksman ME, Marsh SP (1993) Handbook of crystal growth, fundamentals: transport and stability, vol. 1B. Elsevier Science Publishers B.V., New York, pp 1075–1122
22. Keller A (1958) Growth and Perfection of Crystals, Wiley-Interscience, New York, pp 499–532
23. Khoury F, Padden FJ (1960) J Polym Sci 47:455
24. Geil PH, Reneker DH (1961) J Polym Sci 51:569
25. Wunderlich B, Sullivan P (1962) J Polym Sci 61:195
26. Mareau VH, Prud'homme RE (2005) Macromolecules 38(2):398
27. Sakai Y, Imai M, Kaji K, Tsuji M (1996) Macromolecules 29(27):8830
28. Reiter G, Sommer J (2000) J Chem Phys 112(9):4376
29. Wang M, Braun H, Meyer E (2003) Polymer 44:5015
30. Taguchi K, Miyaji H, Izumi K, Hoshino A, Miyamoto Y, Kokawa R (2001) Polymer 42:7443
31. Zhang F, Liu J, Huang H, Du B, He T (2002) Eur Phys J E8:289
32. Lovinger AJ, Cais RE (1984) Macromolecules 17(10):1939
33. Beers KL, Douglas JF, Amis EJ, Karim A (2003) Langmuir 19:3935
34. Ferreiro V, Douglas JF, Warren J, Karim A (2002) Phys Rev E 65:042802–1
35. Ferreiro V, Douglas JF, Warren J, Karim A (2002) Phys Rev E 65:051606–1
36. Ben-Jacob E, Deutscher G, Garik P, Goldenfeld ND, Lareah Y (1986) Phys Rev Lett 57(15):1903
37. Ben-Jacob E, Godbey R, Goldenfeld ND, Koplik J, Levine H, Mueller T, Sander LM (1985) Phys Rev Lett 55(12):1315
38. Brener E, Müller-Krumbhaar H, Temkin D (1992) Europhys Lett 17(6):535
39. Goldenfeld N (1987) J Cryst Growth 84:601
40. Müller-Krumbhaar H, Zimmer M, Ihle T, Saito Y (1996) Physica A 224:322
41. Bisault J, Ryschenkow G, Faivre G (1991) J Cryst Growth 110:889
42. Carr SM, Subramanian KN (1982) J Cryst Growth 60:307
43. Matsuno T, Koishi M (1989) J Cryst Growth 94:798
44. Kurz W, Trivedi R (1990) Acta Metall Mater 38(1):1
45. Keith HD, Padden FJ Jr (1963) J Appl Phys 34(8):2409
46. Keith HD, Padden FJ Jr (1964) J Appl Phys 35(4):1270
47. Bassett DC, Olley RH, al Raheil IAM (1988) Polymer 29:1539
48. Keith HD (1964) J Polym Sci A 2:4339
49. Keith HD, Padden FJ Jr (1987) J Polym Sci Part B: Polym Phys 25:2371
50. Schultz JM (1991) Polymer 32(18):3268
51. Russell TP, Ito H, Wignall GD (1988) Macromolecules 21(6):1703
52. Brener E, Müller-Krumbhaar H, Temkin D (1996) Phys Rev E 54(3):2714
53. Shochet O, Kassner K, Ben-Jacob E, Lipson SG, Müller-Krumbhaar H (1992) Physica A 187:87

54. Bogoyavlenskiy VA, Chernova NA (2000) Phys Rev E 61(2):1629
55. Hutter JL, Bechhoefer J (1999) Phys Rev E 59(4):4342
56. Lamelas FJ, Seader S, Zunic M, Sloane CV, Xiong M (2003) Phys Rev B 67:045414–1
57. Shibkov AA, Golovin YI, Zheltov MA, Korolev AA, Leonov AA (2003) Physica A 319:65
58. Hobbs JK, Hill MJ, Keller A, Barham PJ (1999) J Poly Sci B: Polym Phys 37(22):3188
59. Marand H, Xu JN, Srinivas S (1998) Macromolecules 31(23):8219
60. Alfonso GC, Russell TP (1986) Macromolecules 19(4):1143
61. Barham PJ, Chivers RA, Keller A, Martinez-Salazar J, Organ SJ (1985) J Mater Sci 20(5):1625
62. Okerberg BC, Marand H, Submitted to Physical Review E
63. Jukes PC, Das A, Durell M, Trolley D, Higgins AM, Geoghegan M, Macdonald JE, Jones RAL, Brown S, Thompson P (2005) Macromolecules 38(6):2315
64. For a discussion of the variation of Tg with film thickness, see: Ellison CJ, Mundra MK, Torkelson JM (2005) Macromolecules 38(5):1767
65. Keith HD, Padden FJ Jr (1986) Polymer 27:1463
66. Kovacs AJ, Straupe C, Gonthier A (1977) J Poly Sci: Poly Symp 59:31
67. Khoury F (1966) J Res Natl Bur Stand 70A:29
68. Lotz B, Wittmann JC (1986) J Polym Sci Part B: Polym Phys 24(7):1541
69. Brener E, Müller-Krumbhaar H, Temkin D, Abel T (1998) Physica A 249:73
70. Xu H, Matkar R, Kyu T (2005) Phys Rev E 72:011804–1
71. Ihle T, Müller-Krumbhaar H (1993) Phys Rev Lett 70:3083
72. Marentette JM, Brown GR (1998) Polymer 39(6–7):1405
73. Liu F, Goldenfeld N (1990) Phys Rev A 42(8):5052
74. Okerberg B PhD thesis, Virginia Polytechnic Institute and State University, September 2005